frontiers | Frontiers in Virtual Reality

TYPE Original Research
PUBLISHED 12 February 2026
DOI 10.3389/frvir.2026.1693545

OPEN ACCESS

EDITED BY
Dirk Reiners,
University of Central Florida, United States

REVIEWED BY
Perizat Rakhmetova,
K I Satbayev Kazakh National Research Technical University Institute of Automation and Information Technologies, Kazakhstan
Timur Imankulov,
Al-Farabi Kazakh National University, Kazakhstan
Xuefeng Zhao,
Beijing University of Technology, China

*CORRESPONDENCE
Azamat Yeshmukhametov,
azamat.yeshmukhametov@nu.edu.kz
Darkhan Zholtayev,
darkhan.zholtayev@nu.edu.kz

RECEIVED 27 August 2025
REVISED 21 December 2025
ACCEPTED 13 January 2026
PUBLISHED 12 February 2026

CITATION
Dalabekov A, Akimbay D, Akhmetov T, Zholtayev D and Yeshmukhametov A (2026) Mixed reality based in-pipe inspection. *Front. Virtual Real.* 7:1693545. doi: 10.3389/frvir.2026.1693545

Mixed reality based in-pipe inspection

Almat Dalabekov[1], Dias Akimbay[1], Tolegen Akhmetov[1,2], Darkhan Zholtayev[2,3]* and Azamat Yeshmukhametov[1,3]*

[1]Department of Robotics Engineering, School of Engineering and Digital Sciences, Nazarbayev University, Astana, Kazakhstan, [2]Department of Computer Science, Astana IT University, Astana, Kazakhstan, [3]Laboratory of Advanced Robotics and Mechatronics Systems, Institute of Smart Systems and Artificial Intelligence, Astana, Kazakhstan

Pipelines play a critical role in transporting essential resources that support daily life and industrial operations. The expansion of industrial activity and infrastructure development has historically paralleled the growth of the pipeline sector. However, this growth has introduced substantial challenges, particularly in the areas of timely inspection and maintenance of critical infrastructure. To address these challenges, researchers have proposed a range of robotic and non-invasive solutions for pipeline inspection. In this study, we present a novel pre-maintenance approach that integrates mixed reality (MR) technologies using the Meta Quest Pro VR/AR headset. This method enables detailed visualization and analysis of in-pipe defects prior to physical intervention, enhancing decision-making in maintenance planning. As a result, engineers gain comprehensive insight into defect characteristics and can more accurately determine the appropriate tools and procedures required for effective maintenance.

KEYWORDS

in-pipe inspection, meta quest pro, mixed reality, pre-maintenance, VR/AR integration

1 Introduction

The integrity of pipeline infrastructure is paramount in a multitude of industries, including water distribution, wastewater management, and oil and gas transportation. Regular inspection is critical to ensure the continued safe and efficient operation of these networks, preventing failures that can lead to significant economic losses, environmental damage, and risks to public health Restrepo et al. (2009). Similarly, maintaining the integrity of underground pipelines through regular inspections can prevent leaks, bursts, and other costly damage that disrupt essential utility services. The consistent emphasis across various sectors underscores a fundamental need for reliable and effective inspection technologies Liu and Kleiner (2013). In response to this growing demand, significant strides have been made in robotic solutions tailored specifically for pipeline environments. Autonomous in-pipe inspection robots have become essential for safer, faster and cheaper pipeline maintenance, replacing risky manual or tether-based methods Wu et al. (2023), John and Shafeek (2022). Modern designs combine compact frames, high-resolution cameras, and wireless links to stream real-time data from hazardous, confined spaces Wu et al. (2023), Tang et al. (2022). Early cable-driven tools were slow and range-limited, but advances in sensing, actuation and control now let robots cover long, winding networks with minimal downtime Song and Luo (2022), Ren et al. (2019).

Current platforms fall into several locomotion families. Wall-pressed robots maintain constant contact for traction across varying diameters Singh et al. (2024), while screw-drive

robots convert rotation to linear motion for long, narrow pipes Torajizadeh et al. (2023). Vibration-driven designs shake themselves forward through debris-filled lines Korendiy et al. (2023). Wheeled robots handle tight bends and junctions SuginaElankavi et al. (2024), and multi-wheeled variants distribute weight for smoother travel over uneven interiors Cao et al. (2022). Independently adjustable crawlers extend those ideas to kilometer-scale inspections Zhao et al. (2020).

Adaptability is boosted by spring- or cam-based mechanisms that auto-resize to pipe geometry Rusu and Tatar (2022), and by soft-bodied robots that bend through sharp elbows with minimal damage risk Luna et al. (2025). For large-diameter water mains, rugged modular platforms carry heavy sensor payloads and resist high pressure Jeon et al. (2024). In ferrous pipes, magnetic omni-wheel robots maintain adhesion even under flow surges Thung-Od et al. (2022), while inchworm designs with electromagnetic feet and soft toes crawl stably on slippery slopes Khan et al. (2022). Bio-inspired earthworm and caterpillar gaits further enrich the locomotion toolbox, improving flexibility and energy efficiency Venkateswaran et al. (2019).

Robust navigation relies on real-time motion planning and SLAM; wheeled units use trajectory control to track curved paths Elankavi et al. (2022), and steerable screw-drive robots employ feedback loops to counter internal flow disturbances Tourajizadeh et al. (2020). Multi-sensor fusion—combining visual, ultrasonic, thermal and electromagnetic data—creates dense 3-D maps for defect detection and predictive maintenance Wu et al. (2023); Jeon et al. (2024); Baballe (2022). On-board processors analyze this information *in situ*, reducing the latency between anomaly discovery and operator response Baballe (2022).

Economic and operational drivers favor low-cost platforms built from standard parts Salvatore et al. (2021) and energy-efficient electronics that extend the untethered mission time Tang et al. (2022). Wireless communication protocols guaranty continuous data links despite severe attenuation within pipes Tang et al. (2022); Wu et al. (2023). Meanwhile, miniaturized, modular frames streamline repairs, upgrades, and task-specific sensor swaps Cao et al. (2022).

Comprehensive reviews highlight the rapid convergence of breakthroughs in mechanical, material, and AI John and Shafeek (2022). Future research targets deeper miniaturization, smarter autonomy, harsher-environment resilience and even *in-situ* repair capabilities, aiming for fully self-optimizing robots that safeguard global pipeline assets with unprecedented precision Tang et al. (2022); Ren et al. (2019).

In the context of pipeline maintenance, constructing accurate digital twins and visualizing overlapping pipe networks remains a significant challenge. To address this, several augmented reality (AR)–based solutions have been proposed. Cuperschmid et al. introduced a marker less 3D object–tracking system that recognizes a sink's U-shaped trap in real time and overlays animated, step-by-step assembly or maintenance instructions directly onto the video feed Cuperschmid and Sakamoto (2021). Li et al. and Nguyen et al. demonstrated AR-enabled visualization of subsurface pipe layouts without excavation, integrating strain and stress measurements into an AR-aligned pipe map Li et al. (2023); Nguyen et al. (2023). Tsai et al. developed an automatic pipeline-planning framework for building interiors that can be extended to maintenance workflows Tsai et al. (2022). Finally, Moon et al. explored the use of AR smart glasses for interactive visualization and analysis during inspection tasks Moon et al. (2015). Collectively, these advances underscore the growing potential of AR to improve both the planning and execution of pipeline maintenance operations.

In this study, we propose an end-to-end post-inspection (and potentially pre-maintenance) pipeline in which an in-pipe robot acquires dense geometric information in confined environments using an RGB-D camera (e.g., Intel RealSense) and LiDAR; these measurements are then reconstructed in Unity to produce a 3D model that can serve as a digital representation of the pipe. By leveraging SLAM, the approach is intended to support more accurate localization and metric estimation of anomaly geometry—including foreign objects, hole dimensions, and pipe diameter/length—thereby moving beyond purely qualitative visualization. We also present an initial demonstration of real-time anomaly identification within the AR/VR headset by applying DBSCAN clustering to the reconstructed point-cloud stream, which may enable timely detection of debris and structural defects.

The current study is subject to several practical limitations. In particular, the experiments are conducted in pipes with an inner diameter of approximately 400 mm, and the performance and usability of the proposed sensing–reconstruction–visualization pipeline in substantially smaller (or larger) diameters remains to be validated. Moreover, reliable reconstruction in confined pipes is likely sensitive to occlusions, specular/wet surfaces, and sensor-motion artifacts; thus, reconstruction-grade quality may depend on precise, repeatable robot motion and careful sensor placement/calibration. Finally, the fidelity of anomaly dimension estimates and localization accuracy may degrade under low-texture conditions or when SLAM tracking becomes intermittent, motivating further evaluation across a wider range of pipe materials, geometries (e.g., bends, joints), and operational scenarios.

1.1 Problem statement and research contribution

One of the critical challenges in pipeline maintenance is the repair process, which is often time-consuming, environmentally disruptive, and economically costly. To address this, our research project focuses on preventive strategies and introduces a novel approach to pre-maintenance preparation using augmented reality (AR) and virtual reality (VR) technologies.

The primary contribution of this study is the integration of immersive AR/VR systems into pipeline inspection workflows. The proposed method allows users to remotely inspect a 3D-reconstructed pipeline environment using a head-mounted display with gaze-driven control, eliminating the need for manual robot operation. This supports hands-free, spatially aligned visualization of internal pipe structures before physical intervention. Surface anomalies are detected using real-time image processing based on contour segmentation and clustering, with overlays rendered directly in the user's view. These visual cues enable early identification of structural defects such as cracks or holes, enhancing situational awareness and reducing diagnostic

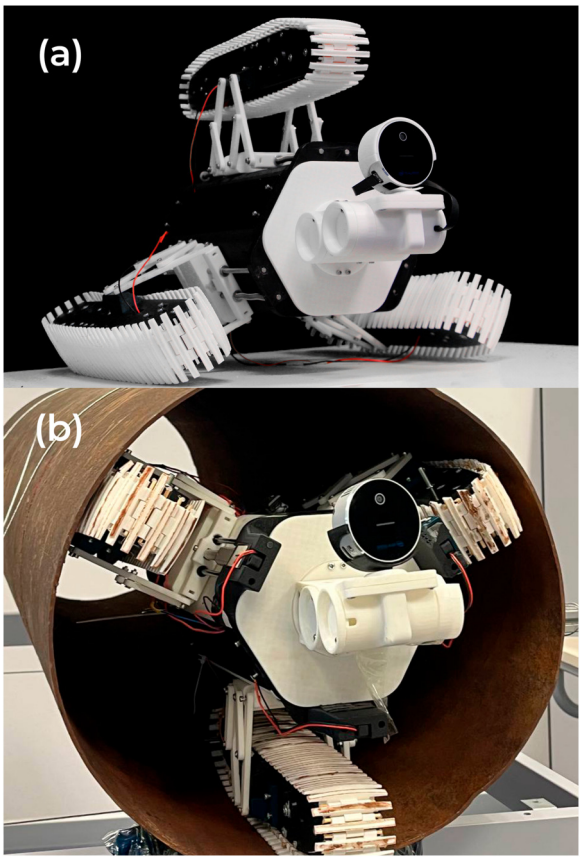

FIGURE 1
(a) Smart in-pipe robot prototype **(b)** Front view.

time. Additionally, interactive virtual tools and a custom spatial ruler provide operators with dimensional analysis capabilities, supporting accurate planning, training, and pre-maintenance decision-making in a safe and immersive environment.

2 Robot design

The developed robot is a hybrid in-pipe inspection system designed for maneuverability and data acquisition within confined pipeline environments (see Figure 1). At the front of the robot, a biaxial-jointed manipulator is integrated, allowing yaw and pitch motions. A RealSense camera is mounted on the end-effector to enable high-resolution visual inspection and mapping.

As illustrated in Figure 2, the central module of the robot connects the manipulator to three mobile chassis and houses critical electronic components. This compartment includes batteries, current sensors, Arduino Uno microcontrollers, motor drivers, a Jetson Orin module, and an NRF communication module, all arranged compactly to optimize space and thermal management.

The locomotion system consists of three independently driven chassis, each equipped with a DC motor. These chassis are positioned 120° apart, ensuring stable and balanced contact with the inner surface of the pipeline. This triangular configuration allows the robot to maintain equilibrium and adapt to varying pipe diameters and orientations during operation.

Each chassis also incorporates an active adjustment mechanism with linear actuators that extend or retract linkages to raise or lower the chassis. This allows the robot to dynamically adapt to different pipe radii. As the actuator-driven links make contact with the inner pipe surface, the current draw increases, which is monitored in real-time by current sensors. Once the current consumption reaches a predefined threshold, indicating firm contact, the system automatically stops the actuator to prevent overexertion or damage. This mechanism ensures precise positioning, and safe interaction with the pipeline structure. Figure 3 shows the difference between passive and active extension mechanisms. Passive mechanism centering alignment directly depends on compression spring constant value and lower part legs springs faces with more pressure rather than upper extension springs. Thus, passive mechanism is far from perfectly centering alignment. Meanwhile, active mechanism can customize the leg length via actuators with current sensor feedback.

3 System design and implementation

In this research, “immersive” refers to an experience in which the user is perceptually and interactively being placed inside the pipeline - not as a passive viewer of images, but as an active inspector who can explore, observe, and even control tools within a 3D pipeline environment using natural head and hand movements.

As shown in Figure 4, the system development followed a structured six-stage pipeline. Initially, physical test objects were positioned within a real pipeline segment. A mobile robot equipped with a depth camera was then deployed to perform multiple scanning passes, capturing the internal structure. The resulting point cloud was processed into a textured three-dimensional (3D) mesh, which was subsequently imported into Unity. The final model was deployed onto the Meta Quest Pro headset, enabling users to observe, measure, and interact with digital representations of the environment in an immersive Mixed Reality (MR) context.

3.1 Physical setup and object placement

The experiment used a 1.5-m long cast iron pipe with a 40 cm interior diameter, mounted horizontally about 50 cm above ground and fixed at both ends. A hybrid in-pipe robot was inserted and remotely controlled for scanning and inspection. To replicate underground conditions, the far end of the pipe was sealed, overhead lighting was turned off, and the robot’s flashlight provided illumination.

Over ten circular holes were drilled into the pipe (three set diagonally as alignment markers) and one localized deformation was made with a hammer, with all defects marked in red tape; for immersive testing a camera, screwdriver, battery cells, and a 3D-printed wheel were placed near the sealed end, and for 3D reconstruction a blue cup and white cube were set 75 cm from the entry so the 50 cm-long robot could fully enter and stabilize before scanning.

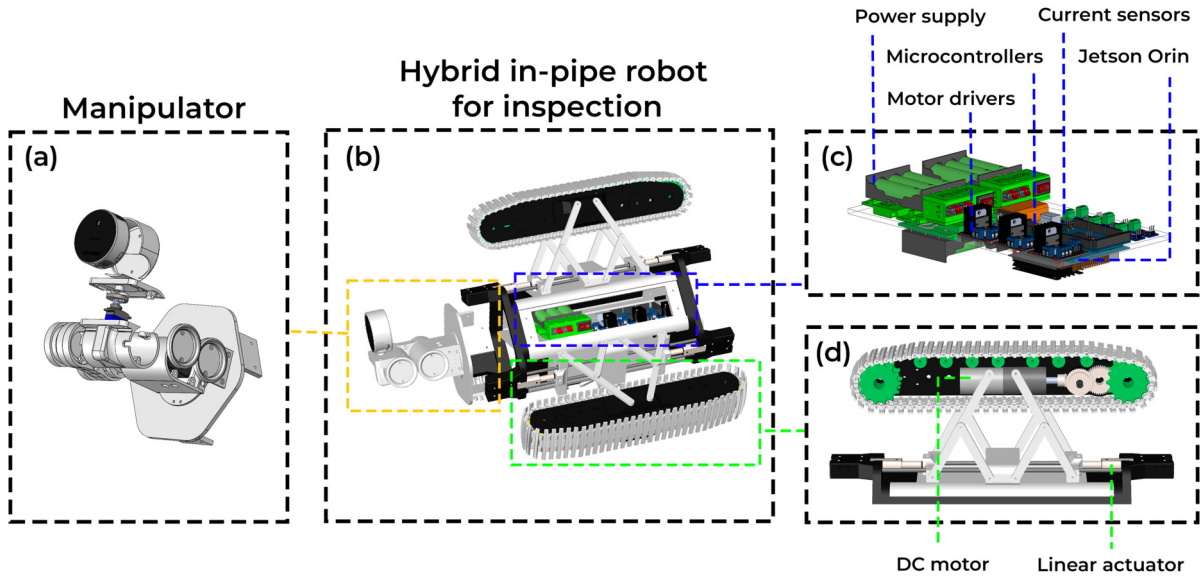

FIGURE 2
(a) Modeling of hybrid in-pipe robot **(b)** 2DOF Manipulator **(c)** Module of electronic devices **(d)** Locomotion module.

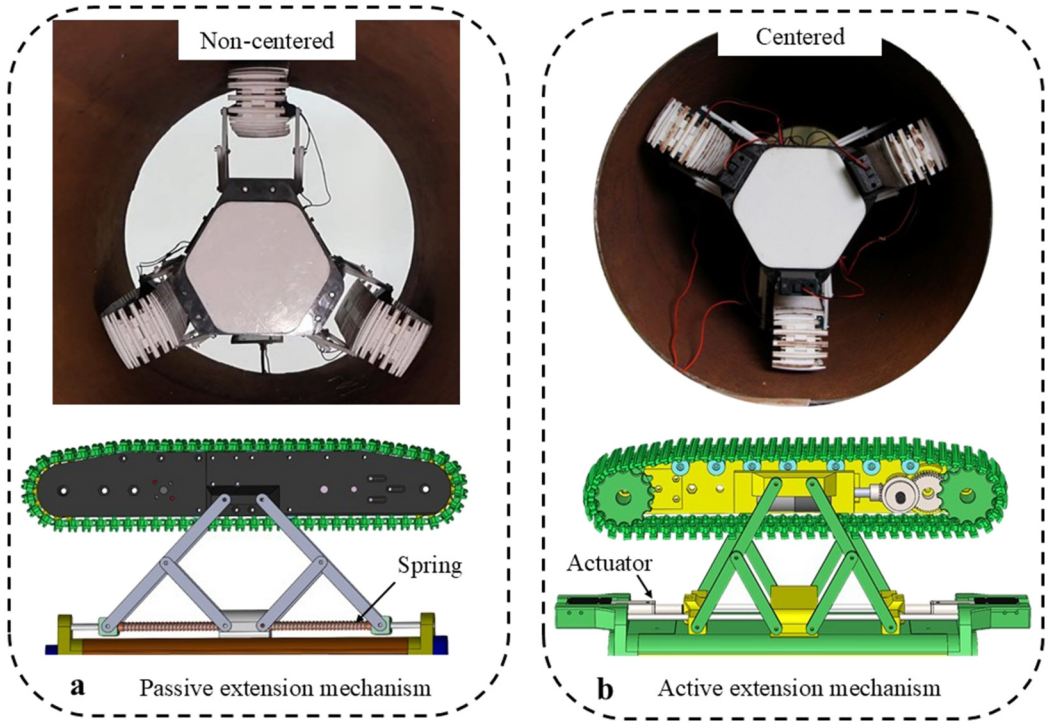

FIGURE 3
(a) Passive extension mechanism **(b)** Active extension mechanism.

3.2 Robot deployment and live immersion mode

The immersive inspection system consists of three tightly integrated components: the robotic platform, a processing and communication unit, and the augmented reality (AR) interface. The overall system architecture and data flow are illustrated in Figure 5, while the operational data flow and closed-loop interaction between control and perception processes during live immersion are depicted in Figure 6. Data-flow representation of the system

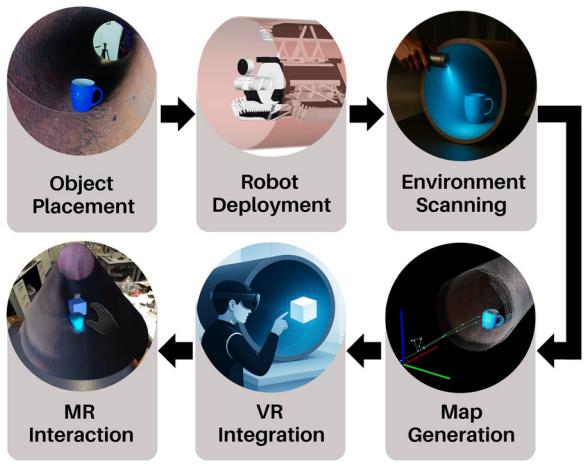

FIGURE 4
Procedure.

highlights the separation between the low-bandwidth gaze-driven control loop and the high-bandwidth visual feedback loop that dominates end-to-end latency.

3.2.1 Robotic subsystem

The mobile robot is based on a differential drive platform and is equipped with an Intel RealSense L515 depth camera mounted on a two-degree-of-freedom pan-tilt mechanism. This configuration enables the acquisition and transmission of RGB, depth, and infrared video streams for real-time inspection. Pan and tilt motions are actuated by servomotors and controlled via an Arduino microcontroller onboard, which receives joint angle commands derived from the user's gaze direction. This setup ensures continuous alignment between the camera orientation and the user's head movements, facilitating responsive and immersive pipeline navigation.

3.2.2 Processing and communication subsystem

Real-time computation is handled by an NVIDIA Jetson Orin NX module, which performs gaze-to-angle transformations, image processing, and data transmission. The user's gaze direction is represented as a three-dimensional vector

$$\mathrm{v} = (x, y, z),$$

obtained from the forward-facing direction of the headset within the Unity virtual coordinate frame. In Unity, the vertical axis corresponds to the y-axis, while the z-axis represents a horizontal forward direction.

To map the virtual gaze direction to the physical orientation of the robot-mounted pan–tilt camera, the gaze vector is decomposed into horizontal and vertical components. The pan angle is computed from the projection of the gaze vector onto the horizontal plane, while the tilt angle is computed from the vertical component using trigonometric relationships (see Figure 7). Because the vertical direction is represented by the y-axis rather than the z-axis in Unity's coordinate convention, the resulting tilt angle is mathematically constrained to the range of -90° to 90° to ensure a valid and unambiguous vertical orientation.

In addition, the camera is mounted horizontally on a two-degree-of-freedom pan–tilt mechanism, which mechanically restricts motion to a single hemispherical workspace. As a result, half of the theoretical pan–tilt configuration space is physically unreachable, and the effective pan angle is further limited by the servo motor's operating range of 180°. These constraints ensure that the computed gaze-driven angles remain consistent with both the virtual coordinate interpretation and the physical limitations of the

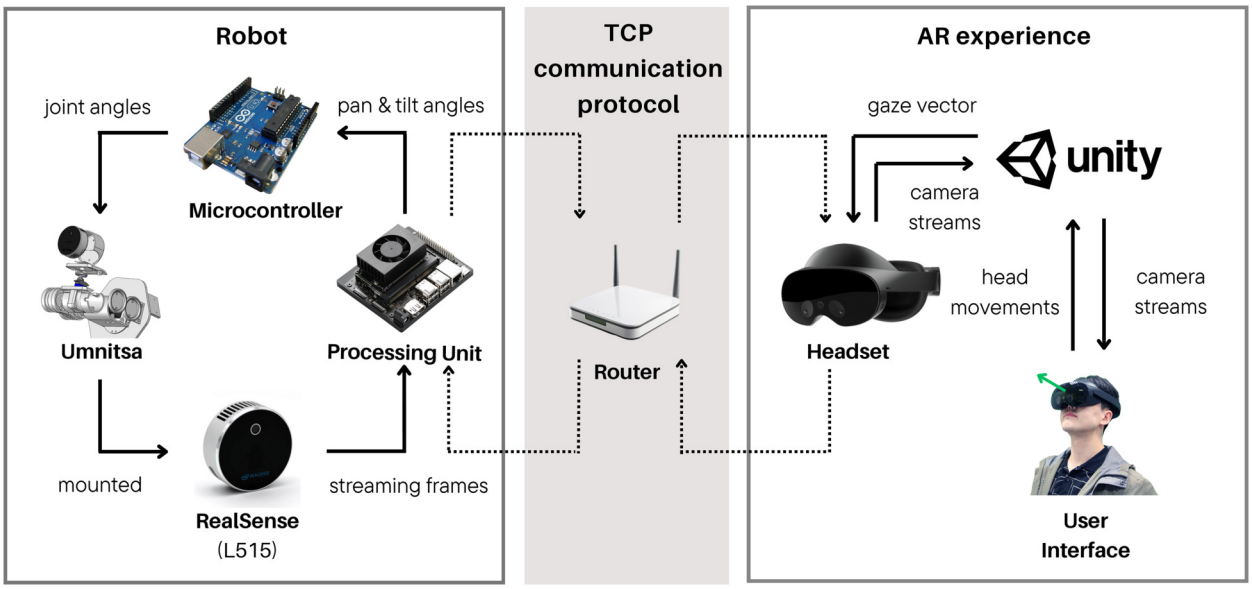

FIGURE 5
System architecture.

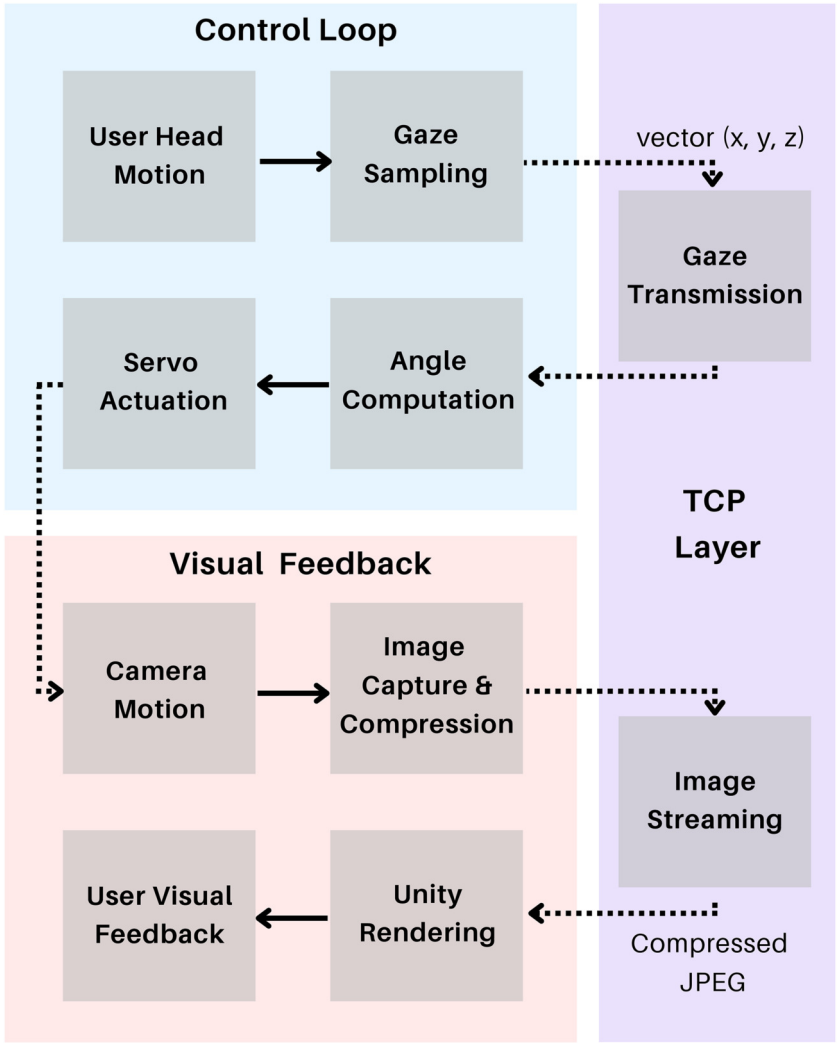

FIGURE 6
Data flow of the MR teleoperation system. The control loop handles low-bandwidth gaze-based commands for camera actuation, whereas the visual feedback loop streams compressed image data to the MR interface and dominates system latency. TCP communication defines the network boundary between control and perception processes.

camera actuation mechanism. The final angles are transmitted to the Arduino microcontroller to actuate the camera's mechanical orientation.

Anomaly detection is conducted using OpenCV for edge and contour extraction, followed by clustering with the DBSCAN algorithm from the scikit-learn library. Each processed video frame is JPEG-compressed and transmitted over TCP to the Unity application running on the MR headset. All communication occurs through a dedicated Wi-Fi router, forming a closed-loop network that synchronizes robot movements and headset feedback in real time.

3.2.3 Augmented reality subsystem

The AR interface is implemented in Unity (version 6000.0.34f1) for the Meta Quest Pro headset using the Meta XR SDK and OpenXR runtime. The application continuously tracks the headset's position and orientation and extracts the forward-facing camera vector to represent the user's gaze direction. This vector is serialized and sent to the Jetson module for computation of the corresponding camera orientation. Although the Meta Quest Pro supports eye-tracking, eye-gaze–based control was not experimentally evaluated in this study, as eye-gaze signals are highly sensitive to involuntary micro-saccades and rapid fixation shifts that can introduce jitter in continuous camera actuation. Head-orientation control was deliberately chosen to provide stable, predictable, and low-noise camera motion during continuous inspection in confined pipe environments.

The robot's camera feed is decoded and dynamically rendered onto a spatially anchored Quad object in Unity using real-time texture mapping. This live projection, aligned with the user's head pose, provides a stereoscopic visual interface of the pipe interior. Integrated overlays enhance the video stream with visualized anomaly clusters, enabling spatially aware, gaze-driven inspection without the need for manual controls.

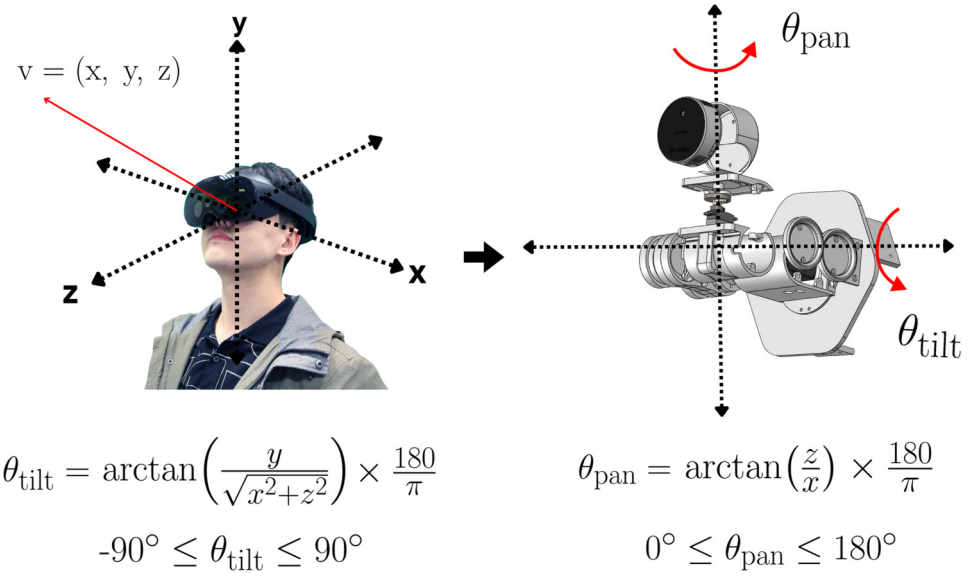

FIGURE 7
Mapping angles.

3.3 Environment scanning and map generation

To evaluate the system's 3D reconstruction capabilities, SLAM-based mapping was performed using an Intel RealSense L515 depth camera mounted at a fixed 90° orientation relative to the pipe's axis. A blue ceramic cup and a white cube were positioned near the midpoint of the 1.5-m cast iron pipe to serve as visual anchors for loop closure. The robot executed multiple forward and reverse passes under RTAB-Map's online mode to increase point cloud density and improve reconstruction fidelity.

3.4 Inspecting pipe with scanned objects

The accumulated point cloud was converted into a polygonal mesh using the Poisson surface reconstruction algorithm with parameters including a target polygon size of 0.03 m, depth 8, and point weight 4.0. The mesh was exported in `.ply` format and subsequently processed in MeshLab to ensure compatibility with Unity. To preserve visual realism, UV coordinates were generated and per-vertex colors were baked into a texture map. The final model was exported in `.obj` format and successfully integrated into Unity for immersive rendering.

3.5 Unity integration

After mesh reconstruction, the pipeline model was placed in a Unity project using the Universal Render Pipeline for XR-friendly lighting and rendering and then deployed to a Meta Quest Pro via the Oculus Integration SDK for stereoscopic, hand- and head-tracked interaction; to mimic maintenance conditions the team added interactive 3D objects such as a screwdriver, hammer, drill and movable cubes, as well as a holographic measurement tool made of two grabbable anchor cubes connected by a dynamic line, with a floating distance label that updates in meters and always faces the user.

3.6 Virtual immersive inspection

In the final stage of implementation, the Unity project was compiled into an Android Package (APK) and deployed to the Meta Quest Pro headset. Upon launch, the application renders a full-scale 3D reconstruction of the pipeline, complete with textured meshes and spatially aligned virtual elements.

Users can freely navigate the virtual environment via hand tracking, enabling them to walk around, enter the pipeline, and interact with digital objects such as test cubes and inspection tools. The integrated measurement tool remains active in this mode, supporting real-time spatial analysis within the immersive scene.

This deployment transforms static mesh data into an interactive MR environment, effectively merging spatial computing with industrial inspection workflows. It enables users to rehearse procedures and assess environments naturally and hands-free, offering practical utility for both training and remote visualization.

To assess the system's functional performance in a real-world scenario, a series of immersive inspection trials were conducted using the final deployed setup. The following section presents the outcomes of these experiments, focusing on camera actuation, gaze tracking, and defect detection within the virtual pipeline environment.

4 Experimental validation

4.1 Live immersion mode

During immersive trials, Meta Quest Pro users steered the robot's pan-tilt camera with natural head movements, keeping

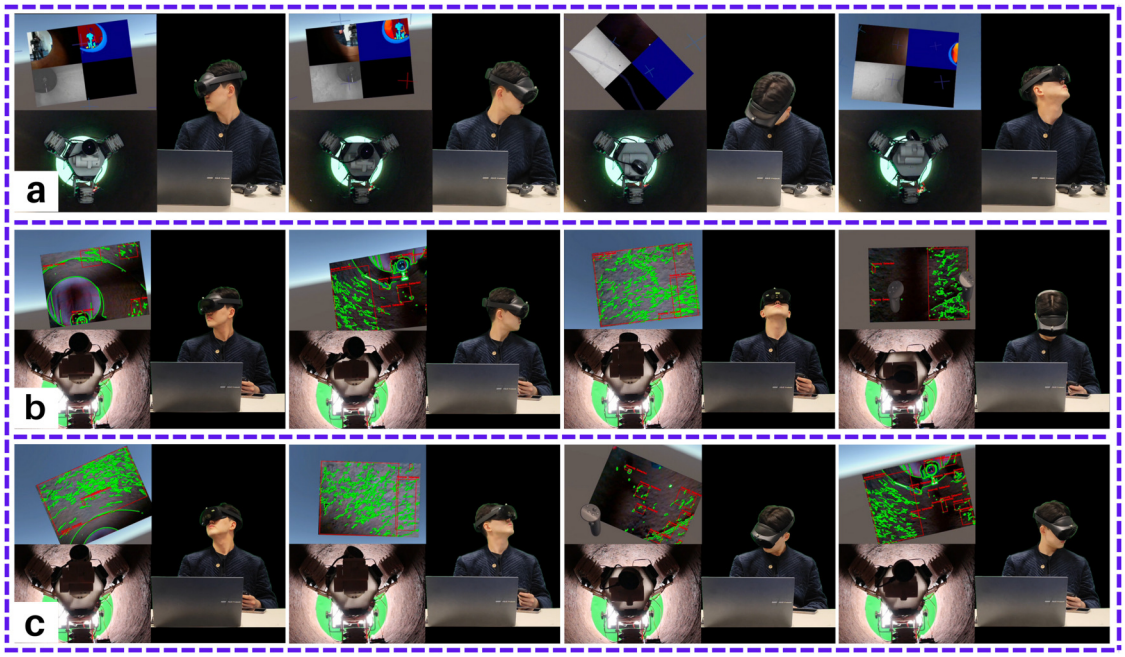

FIGURE 8
Mixed Reality interface and real-time anomaly detection during teleoperation of the Smart In-Pipe Inspection Robot. **(a)** First row: The robot streams synchronized RGB, Depth, and Infrared video to the user's headset. Head movements directly control the robot's gaze (left, right, down-right, up-left). **(b)** Second row: Anomaly detection view highlights pipe surface defects, with gaze-directed inspection (right, left, up, down). **(c)** Third row: Diagonal gaze-controlled inspection showing real-time detection of surface anomalies (up-right, up-left, down-right, down-left).

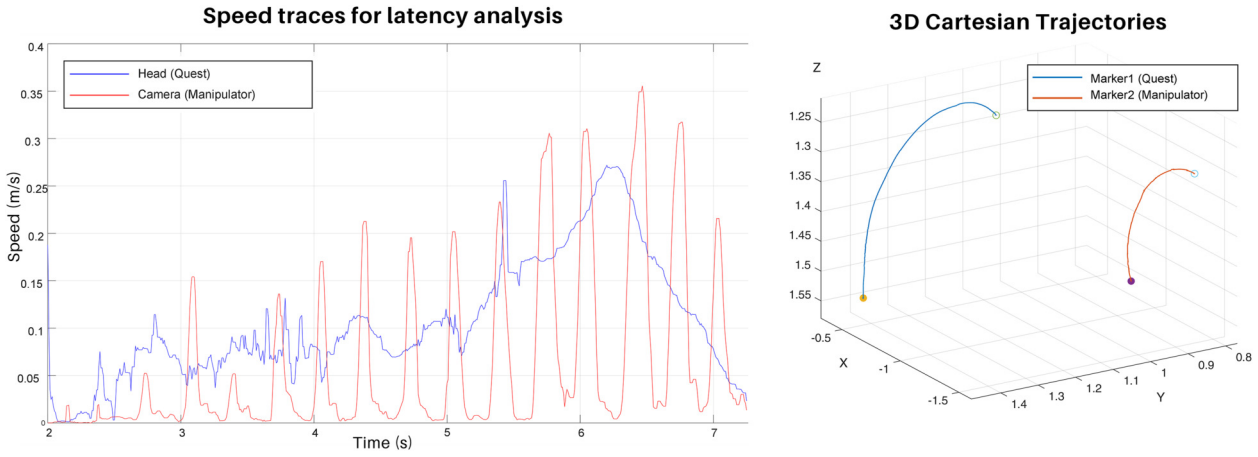

FIGURE 9
Speed traces and 3D trajectories during the teleoperation latency experiment. The left plot shows the smoothed speed profiles of the headset (blue) and the manipulator-mounted camera (red), where the temporal offset between peaks represents the measured delay. The right plot illustrates the corresponding 3D trajectories of both markers captured by the OptiTrack system, showing that the camera followed the user's upward head motion with spatial and temporal consistency.

the view aligned to their gaze for intuitive navigation. Real-time contour segmentation and DBSCAN identified defects and overlaid them onto the video feed, while the overlays remained stable during head or camera motion thanks to synchronized Jetson–Unity–Arduino processing. No perceptible lag was noted, demonstrating the system's real-time responsiveness (see Figure 8).

To quantitatively validate the responsiveness observed during immersive control, a separate experiment was conducted in which the user, equipped with the Meta Quest Pro headset, intentionally performed a distinct upward head motion. The motion of the headset and the corresponding reaction of the robot's pan–tilt camera were captured using the OptiTrack system at 120 Hz, producing two synchronized 3D trajectories (see Figure 9). The temporal relationship between these trajectories was analyzed to estimate the head–camera latency. Let $\mathbf{p}_1(t)$ and $\mathbf{p}_2(t)$ denote the positional signals of the headset and camera markers, respectively,

and $\mathbf{v}_k(t) = \dot{\mathbf{p}}_k(t)$ their velocities. The instantaneous speed magnitudes $s_k(t) = \|\mathbf{v}_k(t)\|$ were smoothed and compared via the normalized cross-correlation function $R_{12}(\tau)$, from which latency was derived as $\tau^* = \text{argmax}_\tau R_{12}(\tau)$. The analysis revealed an average delay of 0.15 ± 0.25 s (approximately 18 frames at 120 Hz), indicating that the manipulator followed the user's head motion with minimal lag. The corresponding speed profiles of both markers are presented in Figure 9, highlighting the temporal offset between movement peaks.

To complement the motion-latency analysis, data transmission and frame rate were evaluated using Python-based logging during live immersion. Each camera frame (raw size ≈3.5 MB) was JPEG-compressed to 25–35 KB before being transmitted from the Jetson to the Unity client. The measured roundtrip times ranged from 0.46 to 0.66 s, corresponding to an effective frame rate of 1.5–2.1 frames per second.

This frame rate reflects bandwidth contention on a shared wireless router, where high-bandwidth image streams and low-latency control commands were transmitted concurrently. As a result, image frames could queue in the communication pipeline despite aggressive compression, while camera actuation commands remained responsive. Importantly, the proposed workflow does not rely on high-frequency visual feedback for camera motion; head-orientation–based control operates through a low-latency pathway (0.15 s head–camera delay), whereas the video stream primarily supports online previewing, defect observation, and path confirmation in a largely static pipe environment.

Consequently, although the visual frame rate is low, the combined results demonstrate real-time responsiveness of the motion control loop and operational adequacy of the video stream for inspection-oriented tasks. Higher frame rates would be required for future extensions involving precise or dynamic teleoperation. Addressing this limitation would require architectural changes at the communication level, which were outside the scope of the present study.

To validate the spatial consistency of the detected anomalies, previously introduced three diagonally positioned holes as alignment markers were used as ground-truth references. These markers enabled comparison between the headset overlays and the actual defect locations on the pipe surface. The Figure 10 shows alignment visualization of one-to-one correspondence between detected virtual clusters and red-taped markers, and confirms the correct coordinate transformation between physical and virtual domains.

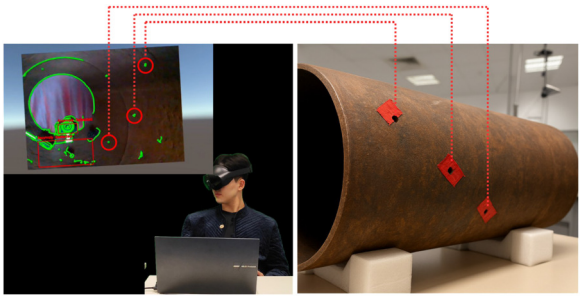

FIGURE 10
Alignment between virtual anomaly detection (left) and real pipe surface (right). The red dotted lines show one-to-one correspondence between detected defects in the headset view and their actual locations on the physical pipe.

4.2 Virtual immersion mode: Initial inspection

Figure 11 presents experimental validation of the virtual immersion mode, focusing on object measurement and simulated maintenance interactions in the Mixed Reality (MR) environment. Column (a) illustrates virtual tools—including a hammer, screwdriver, and drill—measured using a custom-designed holographic ruler. This feature enables users to intuitively estimate object dimensions, supporting potential applications in remote training and procedural planning.

Column (b) demonstrates spatial measurements of the reconstructed pipe. The internal diameter was recorded in both horizontal and vertical orientations, yielding values of approximately 40 cm consistent with the actual pipe's dimensions. The total reconstructed length was around 0.9 m, slightly shorter than the full pipe due to occlusion caused by the robot's body during mapping. Given the robot's length of 40–50 cm, this omission is consistent with expectations.

Columns (c) through (e) depict immersive maintenance scenarios. Each sequence involves entering the pipe, viewing a tool from a first-person perspective, and inspecting designated regions of the pipe wall. In Column (e), a deformed section of the pipe is clearly rendered in the headset. Although no detection algorithm was employed, the geometric irregularity was visually salient. The hammer is directed toward this damaged region to simulate corrective action.

While the tools are grabbable and visually responsive, they are not governed by collision physics and do not interact physically with other virtual objects. As a result, they remain suspended when released. Nonetheless, the system supports intuitive and flexible interaction, enabling immersive workflows for training, inspection, and procedural rehearsal.

Figure 12 presents experimental validation of immersive inspection by combining qualitative spatial exploration with quantitative measurement in the reconstructed pipeline environment.

In the first block (Cube and Cup Comparison), a virtual blue cube was manually placed next to a real ceramic cup to serve as spatial markers. Their physical dimensions were measured using a standard ruler: the cup was 102.8 mm in height and 85.57 mm in diameter, while the cube measured 67.3 mm (height), 116.45 mm (width), and 154.75 mm (length). These values established a ground truth reference for virtual comparisons.

In the second block (Real Object), the same objects were assessed using the virtual ruler inside the Unity environment. The cup was measured as 0.11 m in height and 0.10 m in diameter, while the cube dimensions were 0.17 m (length), 0.14 m (width), and 0.11 m (height). The results show measurable deviations from the real-world values, particularly for smaller objects, indicating potential scaling artifacts and the impact of hand-driven measurement in VR. The virtual ruler

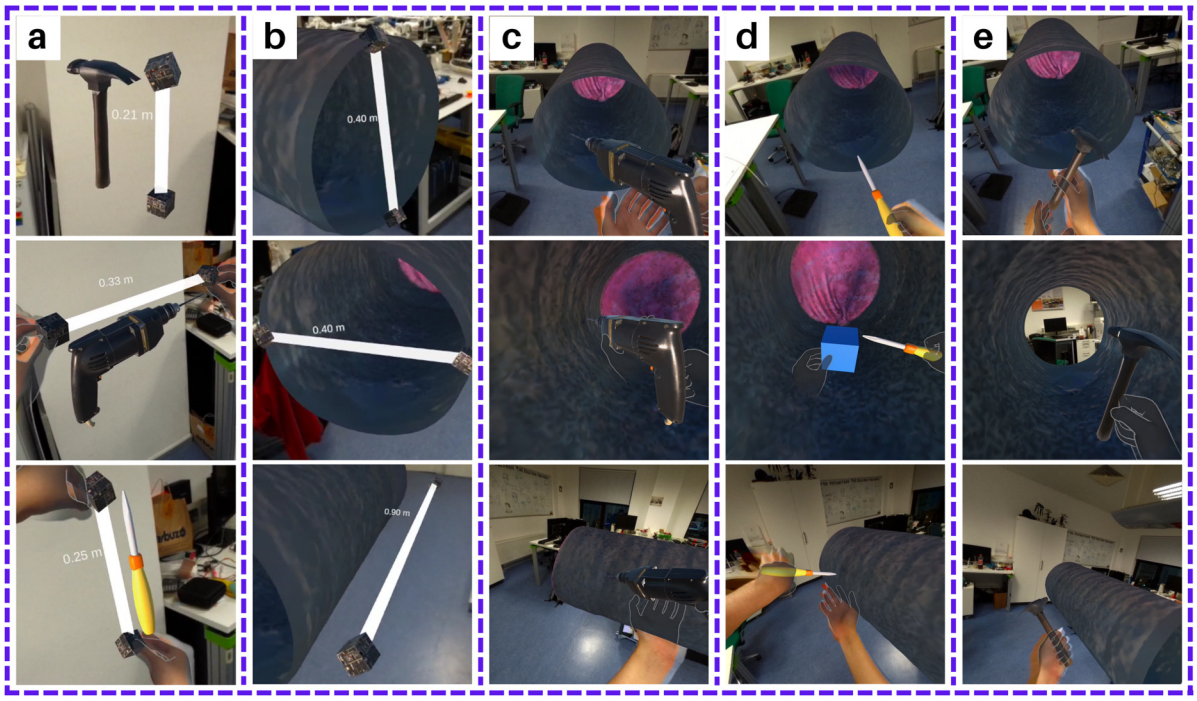

FIGURE 11
Measurement and Interaction. **(a)** Virtual tool-based object measurement using a holographic ruler; **(b)** spatial measurements of the reconstructed pipe; **(c–e)** immersive maintenance inspection sequences inside the pipe environment.

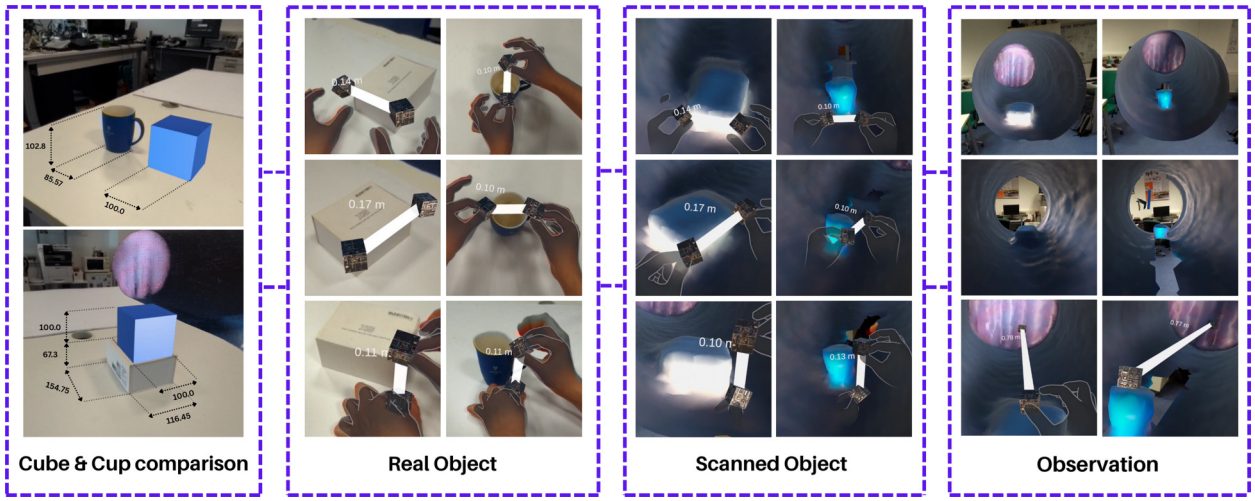

FIGURE 12
Virtual immersion inspection.

was initially designed for medium-to large-scale components, which may contribute to minor inaccuracies when evaluating small items. Nevertheless, more precise measurement is achievable through careful alignment of the anchor points. The cube's proportions appeared visually accurate, supporting intuitive size perception.

The third block (Scanned Object) evaluated the objects as reconstructed in the scanned mesh. The cube dimensions remained unchanged (0.17 × 0.14 × 0.10 m), while the cup's height slightly increased to 0.13 m, with its diameter remaining at 0.10 m. The observed height discrepancy can be attributed to the nature of the mesh reconstruction process. As the objects were

	Cube			Cup	
	Width	Length	Height	Height	Diameter
Real object (VR measurement)	0.17 m	0.14 m	0.11 m	0.11 m	0.10 m
Scanned Object (VR measurement)	0.17 m	0.14 m	0.10 m	0.13 m	0.10 m
Real object (Real measurement)	0.154 m	0.116 m	0.067 m	0.085 m	0.102 m
Mean Error (%)	22-25 %			14 -25 %	

FIGURE 13
Measurement accuracy of cube and cup dimensions comparing VR-based estimation, scanned reconstruction, and real-world ground truth.

placed on the pipe floor, the SLAM system captured only surface point clouds. During Poisson-based mesh generation, the close proximity between the object bases and the pipe surface introduced merged geometry, resulting in unified mesh regions. This geometric blending made it difficult to accurately distinguish vertical boundaries, especially for curved or small items, and may have led to overestimated height values.

To consolidate these observations, the deviations between real-world dimensions, VR-based measurements, and reconstructed mesh values are summarized in Figure 13. For each dimension i, the absolute percentage error was defined as shown in Equation 1:

$$E_i = \frac{|M_i - R_i|}{R_i} \times 100\%, \tag{1}$$

where M_i denotes the measured value (VR or scanned) and R_i is the corresponding real-world measurement. The overall mean error (ME) was then computed as shown in Equation 2:

$$\mathrm{ME} = \frac{1}{n}\sum_{i=1}^{n} E_i, \tag{2}$$

with n representing the number of compared dimensions for each object. As shown in Figure 13, the cube dimensions exhibit mean deviations in the range of 22%–25%, while the cup dimensions remain within 14%–25%.

The fourth block (Observation) highlights spatial coherence within the virtual scene. Front and rear views confirm accurate depth perception and correct object embedding. The far end of the pipe appears sealed, replicating the real experimental setup. Unscanned regions near the cup illustrate occlusion effects caused by the robot's position and limited viewing angles. Unlike the cube, which was shorter and more stable, the cup's taller and narrower shape made it harder to capture fully. Its smaller base increased the likelihood of partial obstruction, resulting in missing floor data around it. The final row of this block includes placement measurements taken from the opposite end of the pipe using the virtual ruler. The recorded positions of the cup and cube were approximately 0.77 m and 0.78 m, respectively, closely matching their real-world setup. This consistency supports the spatial accuracy of reconstructed object placement in the immersive environment.

4.3 Feedback

While the mixed-reality system proved effective for capturing pipe geometry and enabling immersive interaction, several limitations affected scan completeness and measurement precision. During scanning, RTAB-Map's SLAM pipeline was sensitive to platform instability and sudden rotations, particularly from the robot's omni-wheel drive or abrupt pan–tilt movements. Such dynamics reduce feature overlap and introduce motion blur, often leading to tracking loss. Additionally, the pipe's proximity and repetitive, low-texture surfaces degraded stereo depth estimates and reduced mapping robustness. These challenges were compounded by limited onboard processing power, which restricted loop-closure frequency and forced sparser keyframe selection. As a result, some pipe regions remained underexplored or slightly distorted. Smaller structural features (e.g., holes or thin gaps) were also underrepresented due to occlusion or limited camera reach.

These factors contributed to measurement deviations of 14–25 percent, as seen in our comparison of reconstructed models and real-world dimensions. The observed error stems from both SLAM drift and post-processing effects: smoothing in mesh reconstruction can round off edges, while accumulated pose uncertainty skews global shape. Furthermore, the Unity-based virtual measurement tool slightly overestimates distances due to its cursor size and 3D raycasting behavior. To improve performance, we suggest a combination of algorithmic and mechanical enhancements: (i) incorporating IMU data to bridge visual tracking gaps and stabilize orientation; (ii) mechanical damping or smoother scan trajectories to reduce motion artifacts; (iii) near-

range depth sensing for denser sampling in tight spaces; and (iv) increased compute capacity to support more frequent loop closures. Complementary improvements to the virtual measurement interface could also enhance accuracy by enabling more precise point placement. Since the primary objective of the scanning process is to capture overall geometry and dimensional deviations rather than micro-scale perforations, future work will emphasize enhancing surface completeness and mapping accuracy without overfitting to small isolated defects.

The integration of a live immersion mode also enhanced the inspection process. By allowing users to examine the real-world video feed before engaging with the reconstructed model, the system enabled a complementary perspective. This combination of real-time and virtual modes created new opportunities for comparative analysis and validation of spatial alignment. Compared to Li et al. (2023) and Tsai et al. (2022), the proposed mixed-reality system uniquely enables immersive, in-pipe inspection with real-time spatial overlays. While Li et al. (2023) offer a mobile AR system for urban pipes using GPS/RTK to visualize existing pipeline maps, and Tsai et al. (2022) present an AR tool for BIM-based layout planning, both systems operate externally and lack live defect detection or hands-free navigation. In contrast, this proposed headset-based platform performs SLAM-driven 3D reconstruction of the pipe interior, overlays anomalies using real-time segmentation, and supports intuitive, gaze-directed interaction. It requires no predefined markers or external maps, adapts to variable pipe geometries, and delivers high spatial precision, making it more suitable for live defect identification and immersive inspection tasks.

5 Conclusion

This work presents a mixed-reality inspection system integrating a hybrid in-pipe robot with a pan-tilt camera, real-time anomaly overlays, and immersive visualization via the Meta Quest Pro headset. By combining gaze-based control, live video streaming, and spatial reconstruction, the system enables hands-free pipe exploration and intuitive structural assessment.

Experiments confirmed stable camera alignment with head orientation, accurate anomaly overlays, and reliable spatial reconstruction. The Unity-based interface supports object interaction, spatial measurements, and simulated maintenance tasks for inspection rehearsal and scene analysis.

Both quantitative and qualitative evaluations demonstrated the system's effectiveness during live immersive trials. Quantitatively, OptiTrack-based trajectory analysis and software-based frame timing confirmed responsive head–camera coordination and real-time data flow. Qualitatively, users experienced consistent spatial alignment, realistic object scaling, and intuitive interaction despite inherent scanning limitations. The immersive environment successfully replicated key physical features, supporting reliable remote diagnostics, training, and planning tasks.

Future directions include automated defect classification, hand-tracking or haptic feedback for enhanced interactivity, and multimodal fusion to boost realism in live streams. Transitioning from 2D overlays to volumetric or stereoscopic views may further improve awareness and realism.

In conclusion, the system demonstrates the feasibility of integrating mobile robotics with mixed reality for immersive, preemptive pipeline inspection, offering strong potential for industrial diagnostics, operator training, and spatial planning in constrained or hazardous settings.

Data availability statement

The original contributions presented in the study, including supplementary videos, are included in the article and Supplementary Material; further inquiries can be directed to the corresponding authors.

Author contributions

AD: Conceptualization, Methodology, Software, Validation, Writing – original draft, Writing – review and editing. DA: Data curation, Formal Analysis, Investigation, Methodology, Validation, Visualization, Writing – original draft. TA: Conceptualization, Data curation, Methodology, Visualization, Writing – original draft. DZ: Conceptualization, Data curation, Formal Analysis, Visualization, Writing – original draft. AY: Conceptualization, Formal Analysis, Funding acquisition, Investigation, Software, Supervision, Validation, Writing – original draft, Writing – review and editing.

Funding

The author(s) declared that financial support was received for this work and/or its publication. This work was supported by the Science Committee of the Ministry of Education and Science of the Republic of Kazakhstan under Grant No. AP22686767.

Conflict of interest

The author(s) declared that this work was conducted in the absence of any commercial or financial relationships that could be construed as a potential conflict of interest.

Generative AI statement

The author(s) declared that generative AI was not used in the creation of this manuscript.

Any alternative text (alt text) provided alongside figures in this article has been generated by Frontiers with the support of artificial intelligence and reasonable efforts have been made to ensure accuracy, including review by the authors wherever possible. If you identify any issues, please contact us.

Publisher's note

All claims expressed in this article are solely those of the authors and do not necessarily represent those of their

affiliated organizations, or those of the publisher, the editors and the reviewers. Any product that may be evaluated in this article, or claim that may be made by its manufacturer, is not guaranteed or endorsed by the publisher.

Supplementary material

The Supplementary Material for this article can be found online at: https://www.frontiersin.org/articles/10.3389/frvir.2026.1693545/full#supplementary-material

References

Baballe, M. A. (2022). Robotic inspection monitoring system for pipelines. *J. Artif. Intell. Syst.* 4, 50–64. doi:10.33969/ais.2022040104

Cao, E., Tan, H., Bian, Y., Guo, Z., and Zhou, F. (2022). "Design and realization of a 6-wheeled in-pipe robot," in Journal of Physics: Conference Series. Bristol, United Kingdom: IOP Publishing. 2356, 012010, doi:10.1088/1742-6596/2356/1/012010

Cuperschmid, A. R. M., and Sakamoto, M. H. (2021). Augmented reality based on object recognition for piping system maintenance. *J. Archit. Environ. and Struct. Eng. Res.* 4, 38–44. doi:10.30564/jaeser.v4i2.3305

Elankavi, R. S., Dinakaran, D., Doss, A. S. A., Chetty, R. K., and Ramya, M. (2022). Design and motion planning of a wheeled type pipeline inspection robot. *J. Robotics Control (JRC)* 3, 415–430. doi:10.18196/jrc.v3i4.14742

Jeon, K.-W., Jung, E.-J., Bae, J.-H., Park, S.-H., Kim, J.-J., Chung, G., et al. (2024). Development of an in-pipe inspection robot for large-diameter water pipes. *Sensors* 24, 3470. doi:10.3390/s24113470

John, B., and Shafeek, M. (2022). "Pipe inspection robots: a review," in IOP Conference Series: Materials Science and Engineering. Bristol, United Kingdom: IOP Publishing. 1272, 012016, doi:10.1088/1757-899x/1272/1/012016

Khan, M. B., Chuthong, T., Homchanthanakul, J., and Manoonpong, P. (2022). Electromagnetic feet with soft toes for adaptive, versatile, and stable locomotion of an inchworm-inspired pipe crawling robot. *Front. Bioengineering Biotechnology* 10, 842816. doi:10.3389/fbioe.2022.842816

Korendiy, V., Kachur, O., Predko, R., Kotsiumbas, O., Brytkovskyi, V., and Ostashuk, M. (2023). Development and investigation of the vibration-driven in-pipe robot. *Vibroengineering Procedia* 50, 1–7. doi:10.21595/vp.2023.23513

Li, M., Feng, X., Han, Y., and Liu, X. (2023). Mobile augmented reality-based visualization framework for lifecycle o&m support of urban underground pipe networks. *Tunn. Undergr. Space Technol.* 136, 105069. doi:10.1016/j.tust.2023.105069

Liu, Z., and Kleiner, Y. (2013). State of the art review of inspection technologies for condition assessment of water pipes. *Measurement* 46, 1–15. doi:10.1016/j.measurement.2012.05.032

Luna, G. A. A. V., Asaari, M. S. M., Seman, M. T. A., and Din, A. S. (2025). A review on soft in-pipe navigation robot from the perspective of material, structure, locomotion strategy, and actuation technique. *Robotica* 1–27. doi:10.1017/S0263574724001796

Moon, D., Kwon, S., Bock, T., and Ko, H. (2015). "Augmented reality-based on-site pipe assembly process management using smart glasses," in *ISARC. Proceedings of the international symposium on automation and robotics in construction*, 32. doi:10.22260/ISARC2015/0004

Nguyen, L. V., Bui, D. T., and Seidu, R. (2023). Utilization of augmented reality technique for sewer condition visualization. *Water* 15, 4232. doi:10.3390/w15244232

Ren, T., Zhang, Y., Li, Y., Chen, Y., and Liu, Q. (2019). Driving mechanisms, motion, and mechanics of screw drive in-pipe robots: a review. *Appl. Sci.* 9, 2514. doi:10.3390/app9122514

Restrepo, C. E., Simonoff, J. S., and Zimmerman, R. (2009). Causes, cost consequences, and risk implications of accidents in Us hazardous liquid pipeline infrastructure. *Int. J. Crit. Infrastructure Prot.* 2, 38–50. doi:10.1016/j.ijcip.2008.09.001

Rusu, C., and Tatar, M. O. (2022). Adapting mechanisms for in-pipe inspection robots: a review. *Appl. Sci.* 12, 6191. doi:10.3390/app12126191

Salvatore, M. M., Galloro, A., Muzzi, L., Pullano, G., Odry, P., and Carbone, G. (2021). Design of peis: a low-cost pipe inspector robot. *Robotics* 10, 74. doi:10.3390/robotics10020074

Singh, R. P., Dahal, P., Shrestha, S., Shrestha, S., and Mahat, C. (2024). "Design and development of a wall-pressed robot for in-pipe inspection," in IOP Conference Series: Materials Science and Engineering. Bristol, United Kingdom: IOP Publishing. 1314, 012006, doi:10.1088/1757-899x/1314/1/012006

Song, Z., and Luo, Y. (2022). Research status and development trend of oil and gas pipeline robot. *Acad. J. Sci. Technol.* 3, 134–140. doi:10.54097/ajst.v3i3.2914

SuginaElankavi, R., Dinakaran, D., Doss, A. S. A., KuppanaChetty, R., and Ramya, M. (2024). Design of a wheeled-type in-pipe inspection robot to overcome motion singularity in curved pipes. *J. Ambient Intell. Smart Environ.* 16, 43–55. doi:10.3233/ais-220247

Tang, C., Du, B., Jiang, S., Shao, Q., Dong, X., Liu, X.-J., et al. (2022). A pipeline inspection robot for navigating tubular environments in the sub-centimeter scale. *Sci. Robotics* 7, eabm8597. doi:10.1126/scirobotics.abm8597

Thung-Od, K., Kanjanawanishkul, K., Maneewarn, T., Sethaput, T., and Boonyaprapasorn, A. (2022). An in-pipe inspection robot with permanent magnets and omnidirectional wheels: design and implementation. *Appl. Sci.* 12, 1226. doi:10.3390/app12031226

Torajizadeh, H., Asadirad, A., Mashayekhi, E., and Dabiri, G. (2023). Design and manufacturing a novel screw-in-pipe inspection robot with steering capability. *J. Field Robotics* 40, 429–446. doi:10.1002/rob.22136

Tourajizadeh, H., Sedigh, A., Boomeri, V., and Rezaei, M. (2020). Design of a new steerable in-pipe inspection robot and its robust control in presence of pipeline flow. *J. Mech. Eng. Sci.* 14, 6993–7016. doi:10.15282/jmes.14.3.2020.03.0548

Tsai, L.-T., Chi, H.-L., Wu, T.-H., and Kang, S.-C. (2022). Ar-based automatic pipeline planning coordination for on-site mechanical, electrical and plumbing system conflict resolution. *Automation Constr.* 141, 104400. doi:10.1016/j.autcon.2022.104400

Venkateswaran, S., Chablat, D., and Boyer, F. (2019). Numerical and experimental validation of the prototype of a bio-inspired piping inspection robot. *Robotics* 8, 32. doi:10.3390/robotics8020032

Wu, K., Sang, H., Xing, Y., and Lu, Y. (2023). Design of wireless in-pipe inspection robot for image acquisition. *Industrial Robot The International Journal Robotics Research Application* 50, 145–161. doi:10.1108/ir-02-2022-0043

Zhao, W., Zhang, L., and Kim, J. (2020). Design and analysis of independently adjustable large in-pipe robot for long-distance pipeline. *Appl. Sci.* 10, 3637. doi:10.3390/app10103637